



Mass Transfer in Hierarchical Silica Monoliths Loaded With Pt in the Continuous-Flow Liquid-Phase Hydrogenation of *p*-Nitrophenol

Haseeb Ullah Khan Jatoi^{1,2}, Michael Goepel¹, David Poppitz¹, Richard Kohns¹, Dirk Enke¹, Martin Hartmann² and Roger Gläser^{1*}

¹Institute of Chemical Technology, Faculty of Chemistry and Mineralogy, Leipzig University, Leipzig, Germany, ²Erlangen Center for Interface Research and Catalysis, Friedrich-Alexander Universität Erlangen-Nürnberg (FAU), Erlangen, Germany

OPEN ACCESS

Edited by:

Anne Galameau,
UMR5253 Institut de chimie
moléculaire et des matériaux Charles
Gerhardt Montpellier (ICGM), France

Reviewed by:

Pierluigi Barbaro,
National Research Council (CNR), Italy
Hany Elazab,
British University in Egypt, Egypt

*Correspondence:

Roger Gläser
roger.glaeser@uni-leipzig.de

Specialty section:

This article was submitted to
Catalytic Engineering,
a section of the journal
Frontiers in Chemical Engineering

Received: 04 October 2021

Accepted: 17 November 2021

Published: 13 December 2021

Citation:

Jatoi HUK, Goepel M, Poppitz D,
Kohns R, Enke D, Hartmann M and
Gläser R (2021) Mass Transfer in
Hierarchical Silica Monoliths Loaded
With Pt in the Continuous-Flow Liquid-
Phase Hydrogenation of *p*-
Nitrophenol.
Front. Chem. Eng. 3:789416.
doi: 10.3389/fceng.2021.789416

Sol-gel-based silica monoliths with hierarchical mesopores/macropores are promising catalyst support and flow reactors. Here, we report the successful preparation of cylindrically shaped Pt-loaded silica monoliths (length: 2 cm, diameter: 0.5 cm) with a variable mean macropore width of 1, 6, 10, or 27 μm at a fixed mean mesopore width of 17 nm. The Pt-loaded monolithic catalysts were housed in a robust cladding made of borosilicate glass for use as a flow reactor. The monolithic reactors exhibit a permeability as high as 2 μm^2 with a pressure drop below 9 bars over a flow rate range of 2–20 $\text{cm}^3 \text{min}^{-1}$ (solvent: water). The aqueous-phase hydrogenation of *p*-nitrophenol to *p*-aminophenol with NaBH_4 as a reducing agent was used as a test reaction to study the influence of mass transfer on catalytic activity in continuous flow. No influence of flow rate on conversion at a fixed contact time of 2.6 s was observed for monolithic catalysts with mean macropore widths of 1, 10, or 27 μm . As opposed to earlier studies conducted at much lower flow velocities, this strongly indicates the absence of external mass-transfer limitations or stagnant layer formation in the macropores of the monolithic catalysts.

Keywords: hierarchical pore system, silica monolith, flow reactor, mass transfer, platinum catalysis, PNP hydrogenation, test reaction, *p*-nitrophenol

INTRODUCTION

Flow chemistry represents an enabling technology for various chemical transformations that are difficult or impossible to conduct in batch (Baumann et al., 2020) due to multiple advantages, such as realization of high surface-to-volume ratio, efficient mixing, improved heat and mass transfer, and increased selectivity and safety (Plutschack et al., 2017; Akwi and Watts, 2018). One of the widely studied tubular flow reactors is packed bed reactors (PBRs) as they are easy to design and to operate (Perry and Green, 2008). However, PBRs often suffer from problems such as inhomogeneous particle size distribution, high pressure drop, catalyst attrition, maldistribution of fluid, hot spot generation, and creation of stagnant fluid zones (Juan A. Conesa, 2019) (Levenspiel, 1999). In a PBR, the particle size can be reduced to decrease mass-transfer limitations and to increase the available surface area;

Abbreviations: PBR, packed bed reactor; HSM, hierarchical silica monolith; PNP, *p*-nitrophenol; PAP, *p*-aminophenol; MIP, mercury intrusion porosimetry; NP, nanoparticle.

however, in doing so, the overall bed porosity is reduced, resulting in lower permeability and elevated pressure drop. The problem persists even in the case of a PBR consisting of porous particles (Daneyko et al., 2011). Hence, it is difficult to tune the space available for convective mass transfer, the surface area, and the diffusion lengths simultaneously in a packed bed.

Hierarchical mesoporous/macroporous silica monoliths (HSMs) synthesized *via* the sol-gel technique (Lu et al., 2020) possess conducive textural properties such as high porosity and large surface-to-volume ratio for use as catalyst support in flow reactors (Enke et al., 2016; Mrowiec-Białoń et al., 2018). The sol-gel synthesis of HSMs applied to date is derived from the root method, i.e., the so-called Nakanishi procedure, that was originally developed for the preparation of monolithic silica materials for column chromatography applications (Nakanishi and Soga, 1991). The method consists of the sol-gel transition and polymer-assisted phase separation (hydrogel and solvent phases) that results in a fixation of the microporous/macroporous structure by polycondensation of silica oligomers. During alkaline treatment, micropores disappear and mesopores are formed by Ostwald ripening, resulting in a mesoporous/macroporous HSM (Nakanishi et al., 2007). The precise control over the hierarchical arrangement of mesopore and macropore domains in HSM is determined by the conditions of the synthesis procedure. The HSM consists of a porous silica skeleton containing nanoscale intraskeleton mesopores and microscale interskeleton macropore space. The large macropores allow fast advection-dominated mass transfer, while the small mesopores contribute a large surface area for catalyst loading and activity. Macropores provide the deterministic length scale for the bulk fluid flow analogous to the void spaces in a packed bed, while the skeleton thickness defines the diffusion length the same way as the one provided by the particle diameter (Leinweber et al., 2002; Vervoort et al., 2003; Saito et al., 2006; Fletcher et al., 2011; Stoeckel et al., 2015).

A practical advantage of HSMs is that we present a seamless monolith with the physical dimensions of the container within which the gel was dried. In this way, a desired reactor geometry can be realized for flow catalysis by merely hosting the HSM inside a viable cladding material. Owing to the extensively studied surface chemistry and versatility in synthesis steps, HSM supports can be functionalized *via* in situ as well as post-synthesis treatment with a variety of moieties and applied in numerous catalytic applications. Recent studies show successful implementation of silica monolithic catalysts as flow reactors in various chemical and biochemical transformations (El Kadib et al., 2009; Sachse et al., 2010; Linares et al., 2012; Sachse et al., 2012; Sachse et al., 2013; Szymańska et al., 2013; Hakat et al., 2016; Ciemięga et al., 2017; Haas et al., 2017; Liguori et al., 2017; Pélişson et al., 2017; Mrowiec-Białoń et al., 2018; Russell et al., 2020; Yamada et al., 2020; Ahmad et al., 2021; Turke et al., 2021).

However, to make use of the full potential of HSMs as flow reactors, several challenges still have to be overcome. The role of macropore width in relation to diffusion limitations therein and its effect on the catalytic activity have not been studied systematically. This is because the independent tuning of mesopore and macropore widths during the sol-gel synthesis

while maintaining the specific surface area, pore volume, and/or porosity is challenging. The knowledge and general understanding on the macropore width needed to overcome the external, i.e., diffusion limitations within macropores, or stagnant layer formation therein, however, are crucial to enable the key advantage of improved mass transfer in HSMs (as compared to PBRs). Furthermore, it is difficult to wrap a reliably tight cladding around the monolith without compromising its mechanical integrity and restricting fluid bypass. Although the monoliths are hailed as promising reactors in flow applications, most of the studies were reported at low flow rates ($1\text{--}2\text{ cm}^3\text{ min}^{-1}$) and large contact times with very few exceptions (Szymańska et al., 2013). This seriously undermines the advantages of low pressure drop and focuses on mass-transfer investigation in flow conditions not relevant for practical applications. Another reason for this is the absence of a suitable (i.e., intrinsically fast) test reaction to observe the effect of advection-dominated mass transfer in macropores in relation to the catalytic activity at high fluid flow rates ($>5\text{ cm}^3\text{ min}^{-1}$).

This study is aimed to investigate the influence of macropore width on the catalytic activity of Pt-containing HSMs with reference to mass-transfer limitations in a catalytic aqueous-phase conversion in continuous flow. To address these issues, we used a modified synthesis approach to prepare HSMs with a variation of mean macropore width (w_{macro}) but a fixed mean mesopore width (w_{meso}). The other textural properties of the monoliths such as porosity and specific surface area were also fixed in a narrow range. The average skeleton thickness also varied in conjunction to the average macropore width. Borosilicate glass was used as a simple yet versatile cladding material for the synthesized HSM as opposed to largely used materials such as PEEK, heat-shrinkable PTFE, and epoxy resin. To observe the mechanical stability of the cladded monoliths and their hydrodynamic behavior in flow, permeability tests were performed. Various pressure drop–flow rate curves were generated for monoliths of varying w_{macro} to calculate permeabilities as a measure of flow characteristics related to the available macropore space. The dimensionless Reynolds number was calculated to envisage the transport phenomena due to bulk fluid transport in macropores. To investigate the role of monolith textural properties on catalytic activity with respect to mass-transfer limitations, the hydrogenation of *p*-nitrophenol (PNP) to *p*-aminophenol (PAP) using sodium borohydride (NaBH_4) as reducing agent was employed as test reaction (Aditya et al., 2015). Previously, the PNP hydrogenation was successfully used to investigate mass-transfer limitations for Pt- and Pd-loaded catalysts in batch setup (Goepel et al., 2014; Al-Naji et al., 2015). The application of PNP hydrogenation was also investigated in flow microreactors at low flow rates; however, the reaction parameters were challenging to control such as self-hydrolysis of NaBH_4 and the associated bubbling due to hydrogen release that reduced the available catalyst surface (Liu et al., 2017). During catalytic application of Pt-loaded monolithic flow reactors, the role of the variation of w_{macro} was investigated in possible mass-transfer limitations with reference to catalytic activity. Furthermore, the effect of the variation of reactants' volumetric flow rate on catalytic conversion was examined for

probability of stagnant layer formation at the fluid–skeleton interface influencing the mass transfer.

MATERIALS AND METHODS

Chemicals

Sodium borohydride (NaBH_4) ($\geq 96\%$), tetraethyl orthosilicate ($\text{Si}(\text{OC}_2\text{H}_5)_4$) ($\geq 99\%$), and urea ($\text{CH}_4\text{N}_2\text{O}$) ($\geq 99.5\%$) were purchased from Merck (Darmstadt, Germany). Polyethylene oxide (PEO, $-\text{CH}_2\text{CH}_2\text{O}-$) $_n$ (98%, M.W. 100,000 or 100 kDa) and *p*-nitrophenol ($\text{C}_6\text{H}_5\text{NO}_3$) (99%) were purchased from Alfa Aesar (Haverhill, MA), and tetraammineplatinum(II) chloride hydrate ($\text{Pt}(\text{NH}_3)_4\text{Cl}_2\cdot\text{H}_2\text{O}$) (98%) and Pluronic® F-127 were purchased from Sigma-Aldrich (Merck, Darmstadt, Germany). Ammonia (NH_3) (25%) and sulfuric acid (H_2SO_4) (95%) were purchased from VWR International GmbH (Darmstadt, Germany). The deionized water used for solution preparations and aqueous-phase reactions was prepared using PURELAB Flex dispenser by Elga-Veolia (ELGA LabWater, Celle, Germany), with conductivities $< 0.055 \mu\text{S}$. All the chemicals were used as purchased without further purification.

Synthesis of HSMs

The HSMs with mesoporous/macroporous structure were synthesized using an already-established sol-gel procedure using PEO as a structure directing agent and urea as pore controlling agent. Urea proved to be a very suitable pore controlling agent, especially with respect to the mean mesopore width due to homogeneous pore widening during hydrothermal treatment (Kohns et al., 2018). However, to independently alter mean macropore width and to keep the mean mesopore width constant, the present synthesis procedure was modified *via* tuning of the gelation temperature (Meinusch et al., 2017).

The preparation of HSMs is adapted from Kohns et al. (2018). First, 1.8–2.2 g of PEO (M.W. 100 kDa), 2.2 g of urea, and 18 g of deionized water were added under vigorous stirring (in case of Mono-27, 0.5 g Pluronic® F-127 was added too). To this solution, 0.7–1.4 cm^3 of sulfuric acid and 15.5 cm^3 of tetraethyl orthosilicate were added under continuous stirring for 30 min. The reaction mixture turned into a viscous gel, which was poured into polytetrafluoroethylene (PTFE) tubes (7 mm inner diameter and 10 cm length) embedded in a PTFE block. The PTFE block was placed in a steel autoclave (300 cm^3) for gelation at the temperature range of 313–328 K for 24 h. The autoclave was placed in an oven for aging and hydrothermal treatment at 393 K for 20 h. After cooling to room temperature, the wet gels were transferred to a flat trough (volume = 2,000 cm^3) for five to six cycles of washing with distilled water until a neutral pH was obtained (taking approximately 6 h). The gels were dried at 393 K for 24 h by placing them horizontally in plastic vessels covered with water provided with a small leak in their lids resulting in crack-free HSMs (Kohns et al., 2021). The calcination was performed for 8 h with the temperature ramp of 3 K min^{-1} from room temperature to 873 K in a muffle furnace in air atmosphere. This way, four monoliths with constant mean

mesopore width (16–19 nm) and mean macropore widths of 1 μm (2.2 g of PEO, 2.2 g of urea, and 1.4 cm^3 of H_2SO_4 , $T_{\text{gelation}} = 323 \text{ K}$, sample code: Mono-1), 6 μm (2.0 g of PEO, 2.2 g of urea, and 1.4 cm^3 of H_2SO_4 , $T_{\text{gelation}} = 323 \text{ K}$, Mono-6), 10 μm (1.8 g of PEO, 2.2 g of urea, and 1.4 cm^3 of H_2SO_4 , $T_{\text{gelation}} = 323 \text{ K}$, Mono-10), and 27 μm (2.0 g of PEO, 0.5 g of F-127, 2.2 g of urea, and 0.7 cm^3 of H_2SO_4 , $T_{\text{gelation}} = 313 \text{ K}$, Mono-27) were synthesized. The obtained monolithic rods each had the dimensions of 0.5 cm diameter (D) and 9 cm length (L). A paper cutter was used to cut a monolith into the desired length. This allowed for the subsequent use of monoliths in permeability analysis, catalyst loading, and material characterization without losing the shape.

Permeability Test Experiments

The permeability test experiments were performed with the HSM samples containing mean macropore width, $w_{\text{macro}} = 1, 6, 10, \text{ and } 27 \mu\text{m}$, to depict the influence of the varying w_{macro} on the fluid dynamics when pressure-induced flow was applied across the monolith. The monoliths were cut into 2 cm long pieces (diameter = 0.5 cm) using a paper cutter. Each piece was inserted into a borosilicate glass tube with 0.5 cm inner diameter and 0.5 mm wall thickness. The glass was heated with a flame to 1,773 K for ~20 s and then pressed around the monolith. The glass was then allowed to cool at room temperature for ~2–3 min until it took a seamless shape around the monolith external lateral surface. This ensured a tight contact of glass around the monolith without bypass. The glass-cladded monoliths were connected to a FLUSYS™ HPLC pump via Swagelok® Ultra-Torr fitting, and deionized water was used as the transporting fluid. The volumetric flow rate of water was varied over the range 2–20 $\text{cm}^3 \text{ min}^{-1}$ at an increment rate of 2 $\text{cm}^3 \text{ min}^{-1}$. All experiments were conducted at 398 K. The fluid was kept flowing at a specific flow rate until a steady state (i.e., a constant pressure drop) was achieved, and the corresponding pressure drop was measured using an electronic pressure transducer located upstream of the reactor. In case of pressure-driven flow through a porous material such as silica monoliths, the value of permeability (K) was calculated by Darcy's law (Eq. 1) (Bear and Corapcioglu, 1972), where pressure drop (ΔP) across the porous material is a direct function of the fluid volumetric flow rate (q), the fluid viscosity (η), and the length (L) of material in the direction of flow, while it is an indirect function of the cross-sectional area (A) perpendicular to the direction to flow.

$$\Delta p = \frac{q\eta L}{KA} \quad (1)$$

The relationship is essentially a straight line between the flow rate and pressure drop if the flow is laminar. In that case, the slope provides information about the permeability of the material.

Strong Electrostatic Adsorption of Platinum

Before loading, the catalysts (Mono-1, Mono-10, and Mono-27) were pretreated in a vacuum oven at 343 K and 10 kPa for 24 h. The monoliths (0.5 cm diameter and 8 cm length) were then

submerged into 20 cm³ of deionized water in an Erlenmeyer flask. The pH of the deionized water was adjusted to 10 by dropwise addition of 1 M ammonia solution, and the monoliths were kept in this solution for 1 h while stirring at 100 min⁻¹. A 0.1 M aqueous solution of tetraammineplatinum(II) chloride hydrate was added dropwise with an aimed mass fraction of 1.5 wt.-% Pt relative to the mass of the monolith. The solution containing the monolith was stirred for 24 h (100 min⁻¹) with pH readjusted to 10 every 3 h. The Pt-loaded monoliths were taken out, washed with 30 cm³ of deionized water until the pH was neutral, and dried for 48 h at 338 K in air atmosphere. The monoliths were calcined at 423 K for 16 h with flowing air at the flow rate of 70 cm³ min⁻¹. Finally, reduction was performed at 623 K for 4 h at a temperature ramp of 5 K min⁻¹ in 10 vol.-% H₂ in N₂ atmosphere.

Characterization of Monolith Textural Properties

The nitrogen physisorption experiments were performed on BELSORP[®]-miniX (Microtrac Retsch GmbH, Haan, Germany). The samples were pretreated for 24 h at 393 K under vacuum before measurement. The Brunauer–Emmett–Teller (BET) equation was used to calculate the specific surface area ($p/p_0 = 0.05–0.35$). The mercury intrusion porosimetry (MIP) was conducted on a PoreMaster[®] (Quantachrome Instruments, Boynton Beach, FL) from 0.02 to 400 MPa. The mercury contact angle was set at 141°, and a surface tension of 0.48 N m⁻¹ was used for the determination of pore widths, porosity, and specific pore volume. Pore width distribution in MIP was determined using the Washburn equation, assuming cylindrical pores in the software package [SOLID-SOLver of Intrusion Data (Version 1.6.6)]. The standard deviation for the determination of macropore width (w_{macro}) and mesopore width (w_{meso}) is ±10% and ±5%, respectively. Scanning electron microscopy (SEM) was performed using a Leo 1530 device (Zeiss, Oberkochen, Germany). The samples were placed on carbon tabs and glued with silver paste. For conductivity, the samples were sputtered with gold and investigated with a high tension of 5 kV. The monolith sample images were investigated at equal magnification for overall distribution of macropores. The skeleton thickness (w_s) was calculated by taking the average of 100 measurements from the SEM images for each sample.

Catalyst Characterization

The Pt content of all catalysts was determined by optical emission spectroscopy with inductively coupled plasma (ICP-OES) using a Perkin Elmer Optima 8000 instrument (Waltham, USA). The wavelength chosen was 265.954 nm. Quantification was based on external calibrations. Prior to analysis, the solid samples were dissolved in concentrated acids (HCl, HNO₃, and HF), applying microwave digestion. For the determination of Pt content in the core and periphery of the monolith, the outside of the monolith was cut off using a paper cutter up to a reduced diameter of 2.5 mm and then subsequently crushed and analyzed *via* ICP-OES after digestion. The remaining core was then also crushed and analyzed *via* ICP-OES after digestion. Scanning transmission

electron microscopy (STEM) and transmission electron microscopy (TEM) were performed on JEM-2100 Plus (JEOL, Tokyo, Japan) operated at a 200 kV acceleration voltage. An Octane-T-Optima-30 (AMETEK, Berwyn, United States) detector was used for chemical analysis. The samples were mortared in ethanol, and a droplet was transferred to a TEM grid. For TEM tomography, a dual-axis tomography holder model 2040 (Fischione, PA, United States) was used where high tilt angles of ±70° could be achieved. Data reconstruction was performed by IMOD package version 4.11 and segmentation by a thresholding technique. The energy-dispersive X-ray (EDX) analysis was performed *via* a Bruker XFlash 6130 detector at high tension (20 kV), and hydrogen chemisorption was performed on an Autosorb-iQ[®] (Quantachrome Instruments, Boynton Beach, FL, United States).

p-Nitrophenol Hydrogenation in Flow

The Pt-loaded HSM catalysts with mean w_{macro} , 1 and 27 μm, and diameter ($D = 0.5$ cm) were cut into four different lengths ($L = 0.25, 0.5, 1.0,$ and 2.0 cm) and cladded in borosilicate glass (see *Permeability Test Experiments*). The contact time of the reactants in the flow reactor was used as a fixed parameter to investigate the effect of mass-transfer limitations due to the variation of w_{macro} at different volumetric flow rates. A specific flow was maintained for the reactor of a particular length so that the contact time remains the same. For a cylindrical monolithic reactor, the contact time (t_c) was calculated using the following equation:

$$t_c = \frac{\pi r^2 L \varepsilon_T}{q} \quad (2)$$

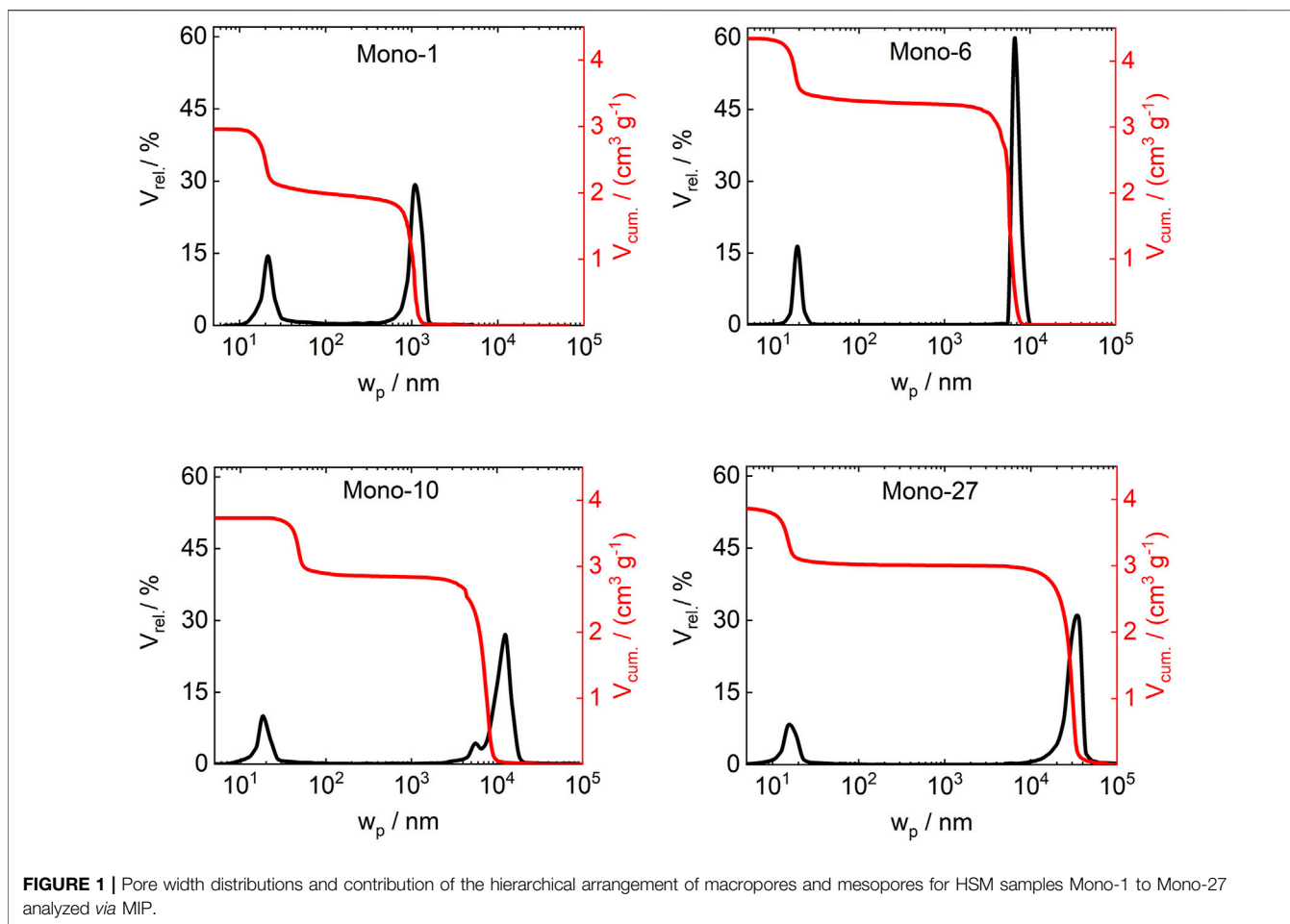
where r is the monolith radius, L is the monolith length, q is the volumetric flow rate, and ε_T is the total porosity. The ε_T was calculated from Eq. 3 using the total pore volume (V_{TP}) determined from MIP (Eq. 4) for the density ($\rho_{Silica} = 2.2$ g cm⁻³) of the silica monolith.

$$\varepsilon_T = V_{TP} / \left(V_{TP} + \frac{1}{\rho_{Silica}} \right) \quad (3)$$

$$V_{TP} = V_{macro} + V_{meso} \quad (4)$$

The flow rates were varied from $q = 1$ to 8 cm³ min⁻¹ corresponding to the lengths of reactors from $L = 0.25$ to 2.0 cm, respectively. In this way, it was possible to observe conversion at steady state for each reactor at a fixed contact time and varying flow rates.

For each reaction run, the freshly prepared aqueous reactant mixture (0.4 mM PNP and 1.6 mM NaBH₄) was pumped through the monolithic reactor. The reaction is reported as pseudo-first order with respect to PNP with an excess reducing agent (Gu et al., 2015). An Avantes (Apeldoorn, the Netherlands) AvaSpec-3648 high-resolution fiber-optic UV-Vis spectrometer with a reflectance-type dip probe was used to monitor the reactant concentration downstream of the reactor (Supplementary Figure S1). The PNP solution is light yellow in color and provides an absorbance peak at a wavelength of 313 nm. However, when aqueous solution of NaBH₄ is added, the PNP

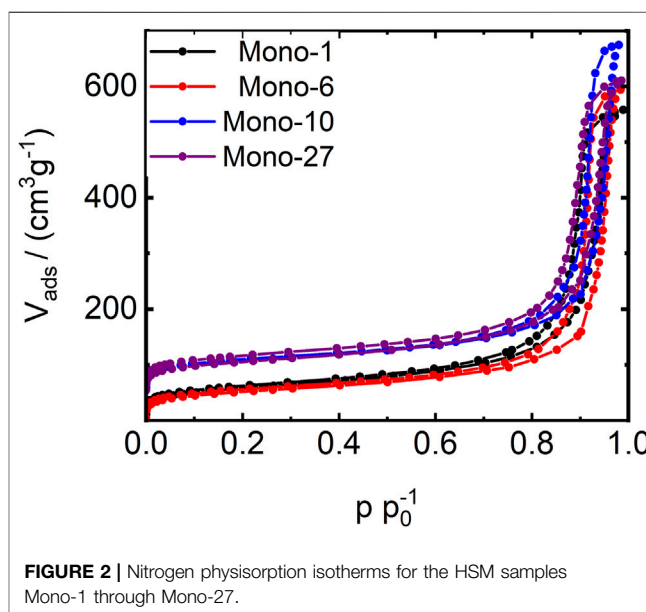


anion is formed along with *in situ* generation of hydrogen. The hydrogenation of PNP to PAP initiates as soon as the reaction mixture comes into contact with a suitable active catalyst such as Pt. The absorbance peak at 400 nm was used for quantification of conversion as given in Goepel et al. (2014). No Pt leaching was observed *via* elemental analysis of the reactor effluent by ICP-OES.

RESULTS AND DISCUSSION

Monolith Synthesis Conditions and Textural Properties

The silica monoliths prepared by the sol-gel procedure possess a seamless, cylindrical morphology without cracks or bends along any physical dimension. Each monolith measures 0.5 cm in diameter and ~9 cm in length. The characterization using MIP shows that each monolithic sample exhibits a bimodal mesoporous/macroporous pore width distribution. A variation of mean macropore width (w_{macro}) in the sequence of 1, 6, 10, and 27 μm is obtained while the mean mesopore width (w_{meso})



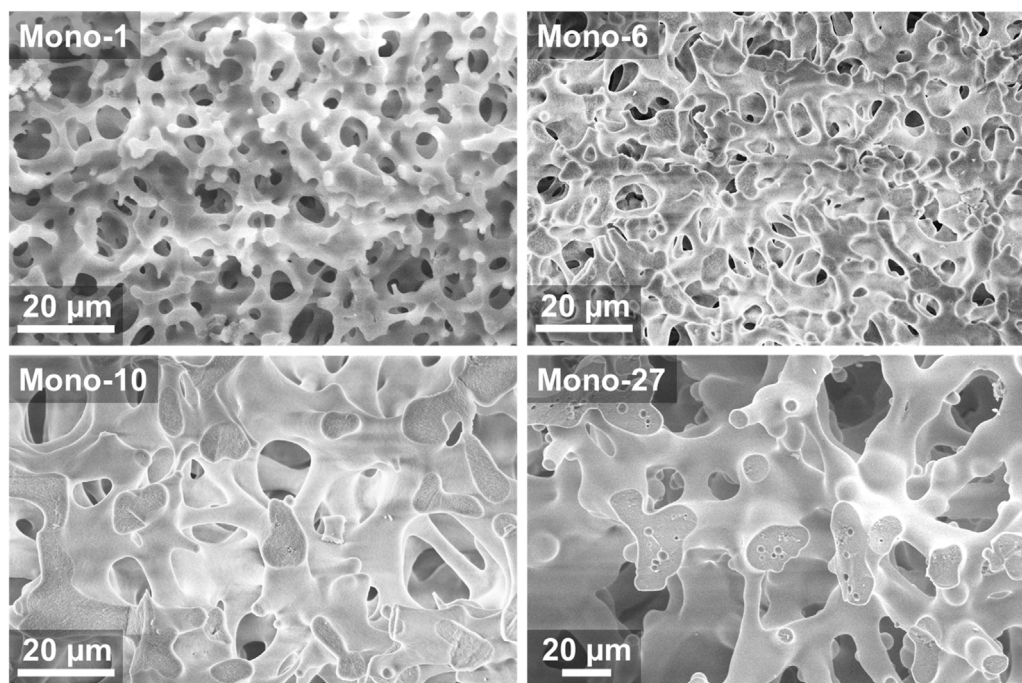


FIGURE 3 | SEM images of HSM samples (Mono-1 through Mono-27) exhibiting the homogeneous arrangement and size of macropores and the growth and thickness of the silica skeleton inside the overall structure.

TABLE 1 | Textural properties [macropore width (w_{macro}), macropore volume (V_{macro}), monolith skeleton thickness (w_s), mesopore width (w_{meso}), mesopore volume (V_{meso}), total porosity (ϵ_T), and BET surface area (S_{BET})] of the synthesized HSMs.

Sample	w_{macro}^a (μm)	V_{macro}^a ($\text{cm}^3 \text{g}^{-1}$)	w_s^b (μm)	w_{meso}^a (nm)	V_{meso}^a ($\text{cm}^3 \text{g}^{-1}$)	ϵ_T^a	S_{BET}^c ($\text{m}^2 \text{g}^{-1}$)
Mono-1	1.00 ± 0.1	2.05	2	19 ± 0.95	0.91	0.87	202
Mono-6	6 ± 0.6	3.42	4	17 ± 0.85	0.91	0.90	195
Mono-10	10 ± 1	2.88	7	18 ± 0.9	0.85	0.89	200
Mono-27	27 ± 2.7	3.03	15	16 ± 0.8	0.83	0.89	196

^afrom MIP.

^bfrom SEM images.

^cfrom nitrogen physisorption.

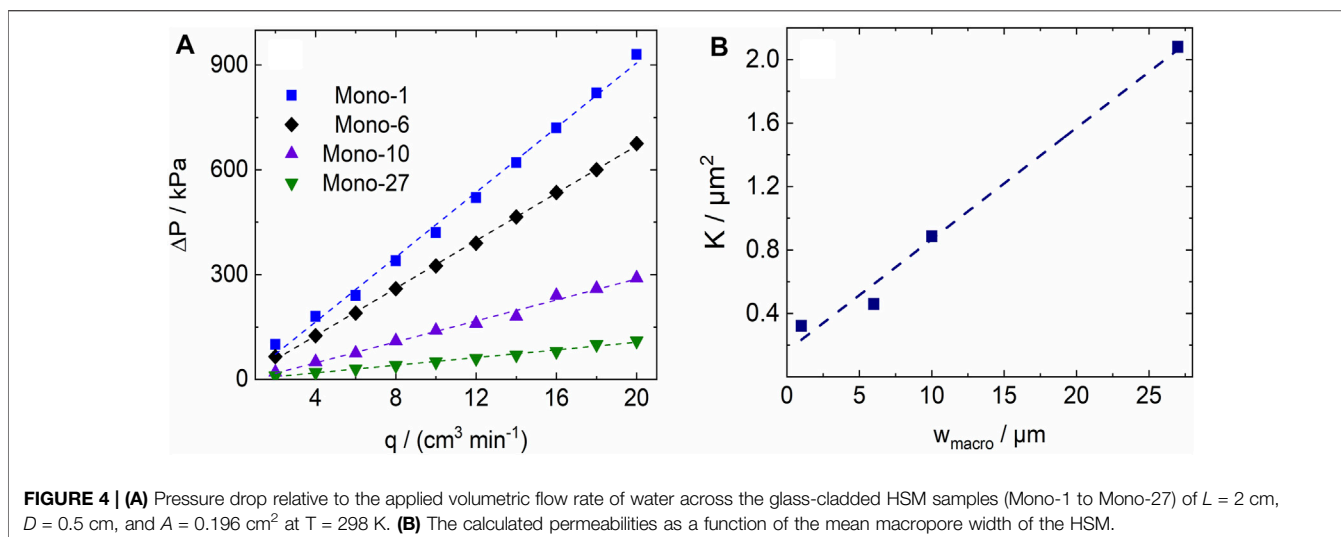
remains in a narrow range of 16–19 nm (Figure 1). The total porosity (ϵ_T) is comparable for all samples in the range of 87%–90%. Also, the specific volumes of the macropore (V_{macro}) and the mesopore (V_{meso}) systems are maintained in the range of 2.05 – $3.42 \text{ cm}^3 \text{g}^{-1}$ and 0.83 – $0.91 \text{ cm}^3 \text{g}^{-1}$, respectively. As expected, the increase in PEO as pore generator systematically decreases the mean macropore width (Kohns et al., 2018). The nitrogen physisorption isotherms (Figure 2) depict Type IV(a) isotherms with hysteresis that are typical of mesoporous material. In each sample, the hysteresis shape is defined by the empirical classification of the H1 type (Schlumberger and Thommes, 2021), suggesting that the monoliths consist of independent cylindrical pores without pore blockage with a three-dimensionally arranged ordered network in the overall sample. The BET surface area for all the monolith samples calculated from the nitrogen physisorption data is in a narrow range of 195 – $202 \text{ m}^2 \text{g}^{-1}$. Since there is no visible plateau

in the physisorption isotherms for all these samples, the mean mesopore width identified by MIP is considered reliable. Nonetheless, there appears to be a convergence at the highest achievable pressure, depicting possibly unique and close values of mean mesopore widths.

The SEM images (Figure 3) show homogeneously distributed macropores throughout the samples separated by the silica skeleton thickness unique to each sample. The skeleton thickness (w_s) increases consistently from 2 to 15 μm with increasing average macropore widths (from 1 to 27 μm). The detailed textural properties of the HSM samples are presented in Table 1.

Flow Characteristics Within the Monolith

With water ($\eta = 0.89 \text{ cP}$ at 298 K) as transporting fluid, all the silica monolith samples (Mono-1 to Mono-27) with dimensions $L = 2 \text{ cm}$, $D = 0.5 \text{ cm}$, and $A = 0.196 \text{ cm}^2$, exhibited a linear



relationship, thus obeying Darcy's law (Figure 4A). This linearity provided a value of permeability for each of the monoliths having a particular mean macropore width considered over the flow rate range 2–20 $\text{cm}^3 \text{min}^{-1}$ (Figure 4B). The permeabilities were 0.32, 0.46, 0.89, and 2.07 μm^2 for samples Mono-1, Mono-6, Mono-10, and Mono-27, respectively. The values of permeability are ideal in terms of application of these monoliths in flow catalysis (Galarneau et al., 2016a). The maximum pressure recorded was only 900 kPa or 9 bar for Mono-1 at 20 $\text{cm}^3 \text{min}^{-1}$. The observed permeabilities suggest mechanically stable and homogeneously distributed macropores (Kohns et al., 2018). When hierarchical monoliths are applied as flow systems, the convective transport in macropores works in conjunction with the diffusive mass transfer in mesopores. Seeking analogy with a packed bed, the dimensionless Reynolds number (Re) is given by the relationship (Leinweber and Tallarek, 2003) (Eq. 5):

$$Re = \frac{u_{sf} w_x}{\nu} \quad (5)$$

where $u_{sf} = \frac{q}{A}$ is the superficial velocity of the fluid in porous medium, w_x is the characteristic length affecting the flow condition (skeleton thickness (w_s) in case of monolith), and ν is the kinematic viscosity of transporting fluid (0.893 $\text{mm}^2 \text{s}^{-1}$ for water at 298 K). For all the monolith samples, Re remains below 1, signifying the retainment of a laminar flow regime over the flow rate range considered. Combining the concept of flow through a straight channel and monolith treated as a packed bed, the Kozeny-Carmen equation (Hormann and Tallarek, 2013) (Eq. 6) provides the equivalent particle size (d_p) of a fictitious bed offering permeability similar to that of the monolith.

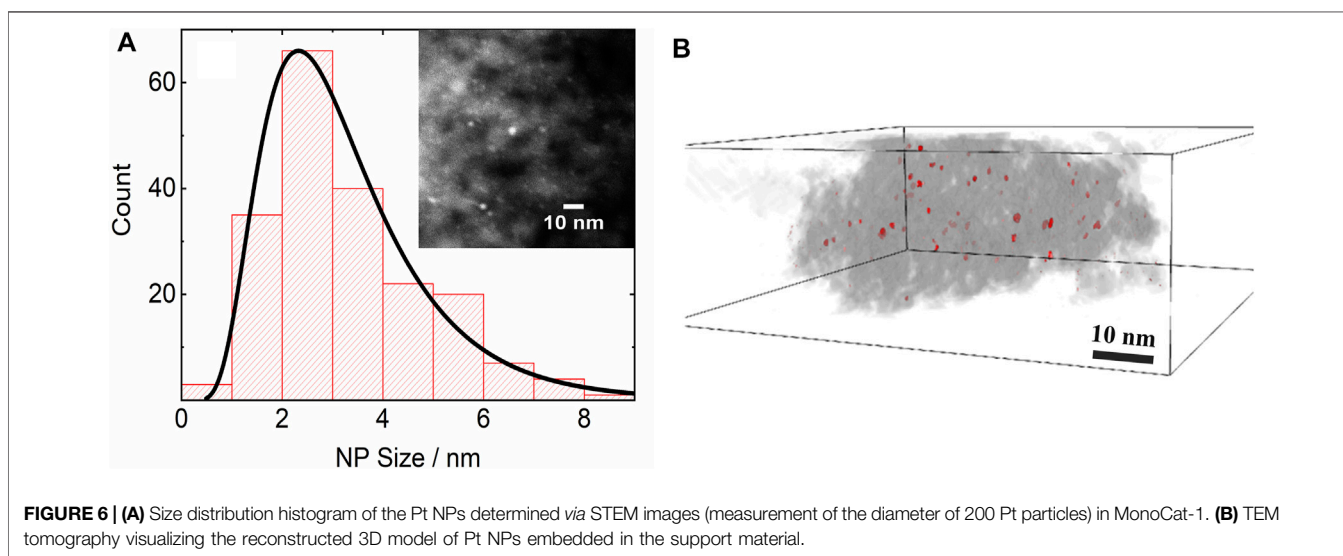
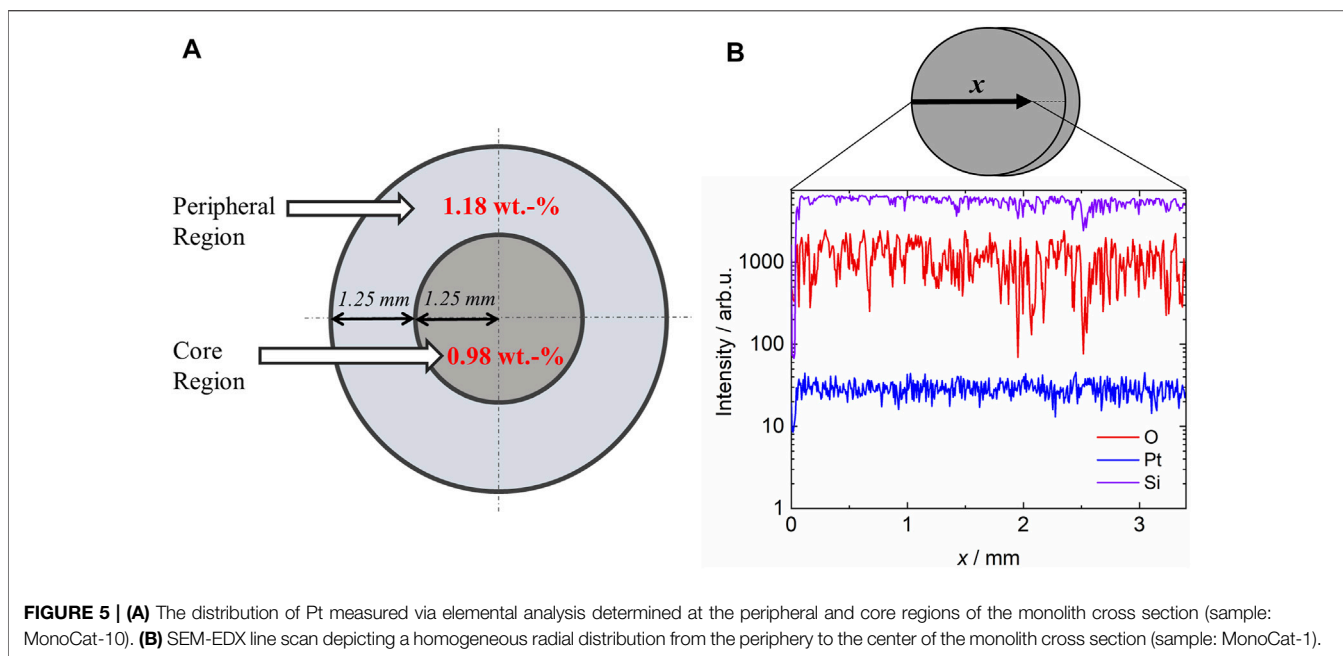
$$u_{sf} = \frac{d_p^2}{180} \frac{\varepsilon p^3}{\eta (1 - \varepsilon p)^2} \frac{\Delta p}{L} \quad (6)$$

For a particulate bed of typical interparticle porosity (ε_p) of 0.36 (Tallarek et al., 2002), a particle size of 20 μm is equivalent to a mean macropore width of 1 μm in the monolith, while a particle

size of 65 μm is equivalent to a 27 μm mean macropore width in a monolith corresponding to the same permeability values. A high permeability maintaining a low pressure drop is technically desirable since it allows the monoliths to operate in a high-flow-rate regime without high cost and mechanical stress that would be caused by high backpressure. The residence time distribution was also investigated for one of the HSM samples (Mono-6) to complement the observed flow behavior. Pulse inputs were given with a 0.5 mM aqueous solution of *p*-nitrophenol as a tracer (Supplementary Figure S2). The residence time distribution for an empty borosilicate glass was compared with one having the monolith inserted in it for volumetric flow rates of 2 and 4 $\text{cm}^3 \text{min}^{-1}$. The distributions completely overlapped each other, exhibiting no indication of maldistribution of the solute due to the presence of the monolith structure. Also, the tailing was observed to be reduced when the flow rate was shifted from a lower to a higher value of flow rate, which indicates a shift towards the ideal plug flow characteristics (Levenspiel, 1999).

Catalyst Characterization and Flow Reactor Configuration

The Pt-loaded HSMs with mean w_{macro} , 1, 10, and 27 μm , were chosen to study the role of the macropore width variation from the smallest to largest values in our samples on the catalytic activity in relation to mass-transfer limitations. The monolithic catalysts and subsequently the reactors hosting these catalysts were interchangeably called MonoCat-1, MonoCat-10, and MonoCat-27 for ease of discussion. The elemental analysis via ICP-OES indicated 1.22, 1.18, and 1.57 wt.-% of Pt in MonoCat-1, MonoCat-10, and MonoCat-27, respectively. The elemental analysis performed at two different sections of the monolith, i.e., the peripheral and the core regions, shows comparable metal loading (periphery: 1.18 wt.-%, core: 0.98 wt.-%) in depth along the monolith diameter for MonoCat-10 (Figure 5A). The SEM-EDX elemental line scan analyzed along the monolith diameter

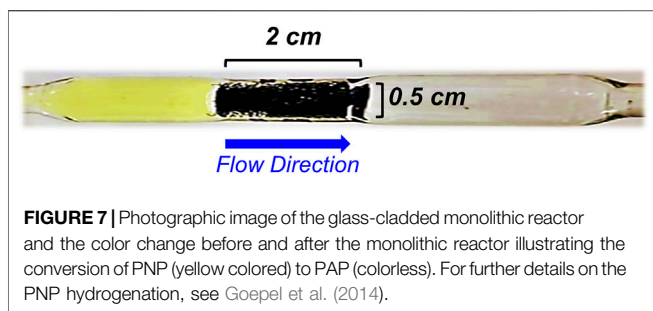


from the periphery towards the center of the monolith also exhibited a homogeneous distribution of Pt along the radial distance for MonoCat-1 (Figure 5B). The platinum nanoparticles (NPs) exhibit a distribution with an arithmetic mean of 3.1 nm as measured from STEM images for MonoCat-1 (Figure 6A). To ensure comparability of the monoliths concerning the Pt NP size, MonoCat-27 was also investigated concerning Pt NP size distribution (Supplementary Figure S3), and a very similar arithmetic mean of 2.6 nm was found. The three-dimensional reconstruction of TEM tomography data indicated a homogeneous distribution of the Pt NPs throughout the image domain (Figure 6B). The average size of the catalytic phase was an order of 8 times below the mean

mesopore width of the monolithic catalyst, indicating that the catalyst was distributed evenly with a narrow size distribution and residing within the monolith skeleton.

Hydrogenation of *p*-Nitrophenol to *p*-Aminophenol in Continuous Flow

The hydrogenation of *p*-nitrophenol (PNP) to *p*-aminophenol (PAP) using sodium borohydride as a reducing agent offers several advantages as a test reaction for catalytic performance of Pt-loaded monolithic catalyst systems: (1) the reaction does not take place in the absence of a catalyst, (2) the reaction occurs in an aqueous phase that is easily accessible in the laboratory and requires no special handling except fresh solution preparation, (3)



the reaction occurs at room temperature and ambient pressure, (4) steady state can usually be achieved in <3 min (**Supplementary Figure S4**), (5) the reaction is intrinsically fast (>70% PNP conversion can be achieved with a contact time <3 s), (6) the color change from the reactant PNP (dark yellow, in the presence of NaBH_4) to the product PAP (colorless) can be easily tracked by simple (online) UV-vis spectroscopy.

Figure 7 illustrates the reactor cladding and the progress of the hydrogenation reaction as well as the UV-vis measurement principle. As a side note, it can be mentioned that glass cladding enables monitoring of the qualitative reaction progress with the naked eye and enables the use of other *in situ* characterization techniques at or in the direct vicinity of the monolithic reactor. Another significant advantage of PNP hydrogenation as a test reaction is the speed at which the steady state could be achieved. It takes only 16 s to attain ~70% conversion at steady state for a reactor of 1 cm length when the volumetric flow rate of the reactant solution is shifted from 0 to $8 \text{ cm}^3 \text{ min}^{-1}$ (**Supplementary Figure S4**). Similarly, a new steady state can be achieved in <1 min as soon as the flow rate is adjusted to a new value. This allows for very fast screening of reaction conditions. Since the glass-cladded reactors can be easily and quickly connected to the tubing of the setup *via* the Swagelok® Ultra-Torr fitting, fast screening of cladded monolithic reactors is also possible. Hence, the hydrogenation of PNP proved to be an inexpensive, fast, and facile test reaction to study the catalytic performance in flow configuration.

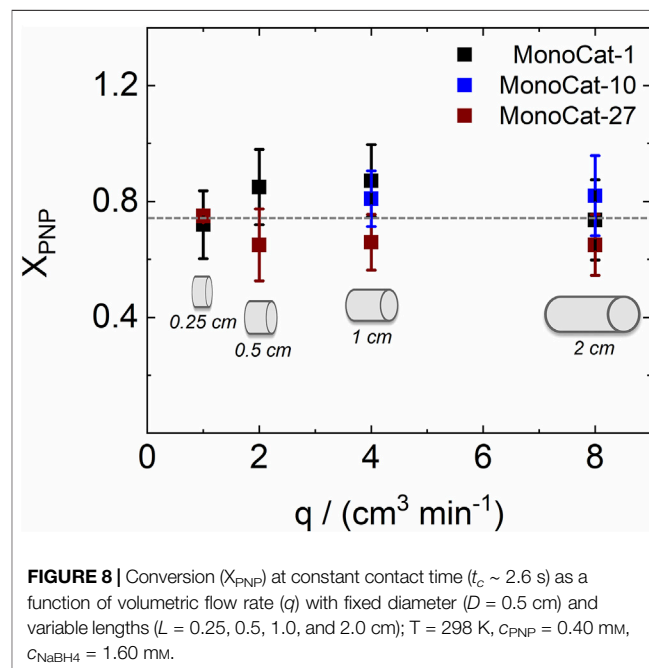
Mass-Transfer Limitations and Catalytic Activity

The monolithic reactors MonoCat-1, MonoCat-10, and MonoCat-27 were applied in the continuous-flow aqueous-phase hydrogenation of PNP to PAP to investigate the influence of mean macropore width on mass-transfer limitations. Prior to these experiments, a linear increase of conversion was observed with an increase in contact time in the flow rate range of $1\text{--}8 \text{ cm}^3 \text{ min}^{-1}$ (**Supplementary Figure S5**), again indicating a homogeneous distribution of reactants and plug flow characteristics in the reactor. To investigate the influence of mass-transfer limitations in macropores, the monolith length and flow rate were varied for the two reactors to keep the contact time constant. This allowed for an investigation into the influence of flow rate or average flow velocity on PNP conversion that was expected to influence the thickness of the stagnant layer formed at the interphase of the monolith skeleton and the bulk fluid. For MonoCat-1 to MonoCat-27, a constant conversion (~75%) at a fixed contact time

(2.6 s) was observed for flow rates between 1 and $8 \text{ cm}^3 \text{ min}^{-1}$ (**Figure 8**). This is a strong indication for the absence of mass-transfer limitations or stagnant-layer formation in the macropores of the monolith. This observation differs from earlier studies (Galarneau et al., 2016b) but may be explained by the different flow rate regimes investigated. The absence of mass-transfer limitations in macropores observed in this work is likely attributed to the high flow rate that could be applied while still achieving measurable conversion due to an intrinsically fast catalytic conversion.

CONCLUSION

Silica monoliths with a variation of macropore width of $1\text{--}27 \mu\text{m}$ and comparable textural properties such as mean mesopore width (17 nm), total porosity (90%), specific surface area ($200 \text{ m}^2 \text{ g}^{-1}$), and specific pore volume ($3 \text{ cm}^3 \text{ g}^{-1}$) were successfully synthesized. The monoliths ($L = 2 \text{ cm}$ and $D = 0.5 \text{ cm}$) exhibit mechanical stability with consistently high permeability (up to $2 \mu\text{m}^2$) over the range of flow rates of $2\text{--}20 \text{ cm}^3 \text{ min}^{-1}$ affiliated to the average macropore width at relatively low pressure drop (1 bar for $27 \mu\text{m}$ at $20 \text{ cm}^3 \text{ min}^{-1}$). Pt was loaded as a catalytically active component with a particle size of $2\text{--}3 \text{ nm}$ embedded homogeneously within the mesopores of the HSM. The aqueous-phase hydrogenation of PNP to PAP was for the first time shown as a facile and fast reaction to investigate the catalytic properties of monolithic catalysts as continuous-flow reactors. Thus, investigations of mass transfer at technically more relevant flow rates are possible due to a fast intrinsic conversion rate. No indication of mass-transfer limitations in macropores was observed for the applied conditions in



contrast to earlier studies. This, again, highlights the potential of superior mass transfer in HSM reactors operated in continuous flow of liquid reaction mixtures.

DATA AVAILABILITY STATEMENT

The raw data supporting the conclusion of this article will be made available by the authors, without undue reservation.

AUTHOR CONTRIBUTIONS

HJ: Experiments (PNP hydrogenation, Pt addition, and flow experiments), manuscript writing. MG: Experiment planning, conception of study, manuscript revision. DP: TEM experiments, manuscript revision. RK: monolith synthesis, monolith textural characterization experiments. DE: Experiment planning (monolith synthesis and characterization), manuscript revision. RG: Experiment planning, manuscript revision, conception of study.

REFERENCES

- Aditya, T., Pal, A., and Pal, T. (2015). Nitroarene Reduction: A Trusted Model Reaction to Test Nanoparticle Catalysts. *Chem. Commun.* 51, 9410–9431. doi:10.1039/c5cc01131k
- Ahmad, S., Sebai, W., Belleville, M.-P., Brun, N., Galarneau, A., and Sanchez-Marcano, J. (2021). Enzymatic Monolithic Reactors for Micropollutants Degradation. *Catal. Today* 362, 62–71. doi:10.1016/j.cattod.2020.04.048
- Akwi, F. M., and Watts, P. (2018). Continuous Flow Chemistry: Where Are We Now? Recent Applications, Challenges and Limitations. *Chem. Commun.* 54, 13894–13928. doi:10.1039/c8cc07427e
- Al-Naji, M., Balu, A. M., Roibu, A., Goepel, M., Einicke, W.-D., Luque, R., et al. (2015). Mechanochemical Preparation of Advanced Catalytically Active Bifunctional Pd-Containing Nanomaterials for Aqueous Phase Hydrogenation. *Catal. Sci. Technol.* 5, 2085–2091. doi:10.1039/C4CY01174K
- Baumann, M., Moody, T. S., Smyth, M., and Wharry, S. (2020). A Perspective on Continuous Flow Chemistry in the Pharmaceutical Industry. *Org. Process. Res. Dev.* 24, 1802–1813. doi:10.1021/acs.oprd.9b00524
- Bear, J., and Corapcioglu, M. Y. (1972). *Dynamics of Fluids in Porous Media*. New York: Dover Publications Inc.
- Ciemiega, A., Maresz, K., Malinowski, J., and Mrowiec-Bialoń, J. (2017). Continuous-Flow Monolithic Silica Microreactors with Arenesulphonic Acid Groups: Structure-Catalytic Activity Relationships. *Catalysts* 7, 255. doi:10.3390/catal7090255
- Conesa, J. A. (2019). *Chemical Reactor Design*. Weinheim, Germany: John Wiley & Sons.
- Daneyko, A., Hölzel, A., Khirevich, S., and Tallarek, U. (2011). Influence of the Particle Size Distribution on Hydraulic Permeability and Eddy Dispersion in Bulk Packings. *Anal. Chem.* 83, 3903–3910. doi:10.1021/ac200424p
- El Kadib, A., Chimenton, R., Sachse, A., Fajula, F., Galarneau, A., and Coq, B. (2009). Functionalized Inorganic Monolithic Microreactors for High Productivity in Fine Chemicals Catalytic Synthesis. *Angew. Chem. Int. Ed.* 48, 4969–4972. doi:10.1002/anie.200805580
- Enke, D., Gläser, R., and Tallarek, U. (2016). Sol-gel and Porous Glass-Based Silica Monoliths With Hierarchical Pore Structure for Solid-Liquid Catalysis. *Chem. Ingenieur Technik* 88, 1561–1585. doi:10.1002/cite.201600049
- Fletcher, P. D. I., Haswell, S. J., He, P., Kelly, S. M., and Mansfield, A. (2011). Permeability of Silica Monoliths Containing Micro- and Nano-Pores. *J. Porous Mater.* 18, 501–508. doi:10.1007/s10934-010-9403-3

FUNDING

This work was supported by the Higher Education Commission (HEC) of Pakistan under the programme Faculty Development for Ph.D. Candidates (Pakistan), 2018 (ID: 57435474) in collaboration with the German Academic Exchange Service (DAAD).

ACKNOWLEDGMENTS

The author(s) acknowledge support from the German Research Foundation (DFG) and Universität Leipzig within the program of Open Access Publishing.

SUPPLEMENTARY MATERIAL

The Supplementary Material for this article can be found online at: <https://www.frontiersin.org/articles/10.3389/fceng.2021.789416/full#supplementary-material>

- Galarneau, A., Abid, Z., Said, B., Didi, Y., Szymanska, K., Jarzębski, A., et al. (2016a). Synthesis and Textural Characterization of Mesoporous and Meso-/Macroporous Silica Monoliths Obtained by Spinodal Decomposition. *Inorganics* 4, 9. doi:10.3390/inorganics4020009
- Galarneau, A., Sachse, A., Said, B., Pelisson, C.-H., Boscaro, P., Brun, N., et al. (2016b). Hierarchical Porous Silica Monoliths: A Novel Class of Microreactors for Process Intensification in Catalysis and Adsorption. *Comptes Rendus Chim.* 19, 231–247. doi:10.1016/j.crci.2015.05.017
- Goepel, M., Al-Naji, M., With, P., Wagner, G., Oeckler, O., Enke, D., et al. (2014). Hydrogenation of *o*-Nitrophenol to *p*-Aminophenol as a Test Reaction for the Catalytic Activity of Supported Pt Catalysts. *Chem. Eng. Technol.* 37, 551–554. doi:10.1002/ceat.201300731
- Gu, S., Lu, Y., Kaiser, J., Albrecht, M., and Ballauff, M. (2015). Kinetic Analysis of the Reduction of 4-Nitrophenol Catalyzed by Au/Pd Nanoalloys Immobilized in Spherical Polyelectrolyte Brushes. *Phys. Chem. Chem. Phys.* 17, 28137–28143. doi:10.1039/c5cp00519a
- Haas, C. P., Müllner, T., Kohns, R., Enke, D., and Tallarek, U. (2017). High-Performance Monoliths in Heterogeneous Catalysis With Single-phase Liquid Flow. *React. Chem. Eng.* 2, 498–511. doi:10.1039/C7RE00042A
- Hakat, Y., Kotbagi, T. V., and Bakker, M. G. (2016). Silver Supported on Hierarchically Porous SiO₂ and Co₃O₄ Monoliths: Efficient Heterogeneous Catalyst for Oxidation of Cyclohexene. *J. Mol. Catal. A: Chem.* 411, 61–71. doi:10.1016/j.molcata.2015.10.015
- Hormann, K., and Tallarek, U. (2013). Analytical Silica Monoliths with Submicron Macropores: Current Limitations to a Direct Morphology-Column Efficiency Scaling. *J. Chromatogr. A* 1312, 26–36. doi:10.1016/j.chroma.2013.08.087
- Kohns, R., Anders, N., Enke, D., and Tallarek, U. (2021). Influence of Pore Space Hierarchy on the Efficiency of an Acetylcholinesterase-Based Support for Biosensors. *Adv. Mater. Inter.* 8, 2000163. doi:10.1002/admi.202000163
- Kohns, R., Haas, C. P., Hölzel, A., Splith, C., Enke, D., and Tallarek, U. (2018). Hierarchical Silica Monoliths With Submicron Macropores as Continuous-Flow Microreactors for Reaction Kinetic and Mechanistic Studies in Heterogeneous Catalysis. *React. Chem. Eng.* 3, 353–364. doi:10.1039/C8RE00037A
- Leinweber, F. C., Lubda, D., Cabrera, K., and Tallarek, U. (2002). Characterization of Silica-Based Monoliths With Bimodal Pore Size Distribution. *Anal. Chem.* 74, 2470–2477. doi:10.1021/ac011163o
- Leinweber, F. C., and Tallarek, U. (2003). Chromatographic Performance of Monolithic and Particulate Stationary Phases. *J. Chromatogr. A* 1006, 207–228. doi:10.1016/S0021-9673(03)00391-1

- Levenspiel, O. (1999). *Chemical Reaction Engineering*. New York, Unites States: John Wiley & Sons.
- Liguori, F., Barbaro, P., Said, B., Galarneau, A., Santo, V. D., Passaglia, E., et al. (2017). Unconventional Pd@sulfonated Silica Monoliths Catalysts for Selective Partial Hydrogenation Reactions Under Continuous Flow. *ChemCatChem*. 9, 3245–3258. doi:10.1002/cctc.201700381
- Linares, N., Hartmann, S., Galarneau, A., and Barbaro, P. (2012). Continuous Partial Hydrogenation Reactions by Pd@unconventional Bimodal Porous Titania Monolith Catalysts. *ACS Catal.* 2, 2194–2198. doi:10.1021/cs3005902
- Liu, A., Yang, L., Traulsen, C. H.-H., and Cornelissen, J. J. L. M. (2017). Immobilization of Catalytic Virus-Like Particles in a Flow Reactor. *Chem. Commun.* 53, 7632–7634. doi:10.1039/c7cc03024j
- Lu, X., Hasegawa, G., Kanamori, K., and Nakanishi, K. (2020). Hierarchically Porous Monoliths Prepared via Sol-Gel Process Accompanied by Spinodal Decomposition. *J. Sol-gel Sci. Technol.* 95, 530–550. doi:10.1007/s10971-020-05370-4
- Meinusch, R., Ellinghaus, R., Hormann, K., Tallarek, U., and Smarsly, B. M. (2017). On the Underestimated Impact of the Gelation Temperature on Macro- and Mesoporosity in Monolithic Silica. *Phys. Chem. Chem. Phys.* 19, 14821–14834. doi:10.1039/c7cp01846k
- Mrowiec-Białoń, J., Ciemięga, A., Maresz, K., Szymańska, K., Pudło, W., and Jarzębski, A. B. (2018). Review on Hierarchically Microstructured Monolithic Reactors for High Yield Continuous Production of fine Chemicals. *Chem. Process. Eng.* 39, 367–375. doi:10.24425/122957
- Nakanishi, K., and Soga, N. (1991). Phase Separation in Gelling Silica-Organic Polymer Solution: Systems Containing Poly(sodium Styrenesulfonate). *J. Am. Ceram. Soc.* 74, 2518–2530. doi:10.1111/j.1151-2916.1991.tb06794.x
- Nakanishi, K., Tanaka, N., Nakanishi, K., and Tanaka, N. (2007). Sol-Gel With Phase Separation. Hierarchically Porous Materials Optimized for High-Performance Liquid Chromatography Separations. *Acc. Chem. Res.* 40, 863–873. doi:10.1021/ar600034p
- Pélisson, C.-H., Nakanishi, T., Zhu, Y., Morisato, K., Kamei, T., Maeno, A., et al. (2017). Grafted Polymethylhydrosiloxane on Hierarchically Porous Silica Monoliths: A New Path to Monolith-Supported Palladium Nanoparticles for Continuous Flow Catalysis Applications. *ACS Appl. Mater. Inter.* 9, 406–412. doi:10.1021/acsami.6b12653
- Perry, R. H., and Green, D. W. (2008). *Perry's Chemical Engineers' Handbook*. New York: McGraw-Hill.
- Plutschack, M. B., Pieber, B., Gilmore, K., and Seeberger, P. H. (2017). The Hitchhiker's Guide to Flow Chemistry. *Chem. Rev.* 117, 11796–11893. doi:10.1021/acs.chemrev.7b00183
- Russell, M. G., Veryser, C., Hunter, J. F., Beingessner, R. L., and Jamison, T. F. (2020). Monolithic Silica Support for Immobilized Catalysis in Continuous Flow. *Adv. Synth. Catal.* 362, 314–319. doi:10.1002/adsc.201901185
- Sachse, A., Galarneau, A., Di Renzo, F., Fajula, F., and Coq, B. (2010). Synthesis of Zeolite Monoliths for Flow Continuous Processes. The Case of Sodalite as a Basic Catalyst. *Chem. Mater.* 22, 4123–4125. doi:10.1021/cm1014064
- Sachse, A., Hulea, V., Finiels, A., Coq, B., Fajula, F., and Galarneau, A. (2012). Alumina-Grafted Macro-/Mesoporous Silica Monoliths as Continuous Flow Microreactors for the Diels-Alder Reaction. *J. Catal.* 287, 62–67. doi:10.1016/j.jcat.2011.12.003
- Sachse, A., Linares, N., Barbaro, P., Fajula, F., and Galarneau, A. (2013). Selective Hydrogenation over Pd Nanoparticles Supported on a Pore-Flow-Through Silica Monolith Microreactor With Hierarchical Porosity. *Dalton Trans.* 42, 1378–1384. doi:10.1039/c2dt31690k
- Saito, H., Nakanishi, K., Hirao, K., and Jinnai, H. (2006). Mutual Consistency between Simulated and Measured Pressure Drops in Silica Monoliths Based on Geometrical Parameters Obtained by Three-Dimensional Laser Scanning Confocal Microscope Observations. *J. Chromatogr. A*. 1119, 95–104. doi:10.1016/j.chroma.2006.03.087
- Schlumberger, C., and Thommes, M. (2021). Characterization of Hierarchically Ordered Porous Materials by Physisorption and Mercury Porosimetry—A Tutorial Review. *Adv. Mater. Inter.* 8, 2002181. doi:10.1002/admi.202002181
- Stoeckel, D., Kübel, C., Loeh, M. O., Smarsly, B. M., and Tallarek, U. (2015). Morphological Analysis of Physically Reconstructed Silica Monoliths With Submicrometer Macropores: Effect of Decreasing Domain Size on Structural Homogeneity. *Langmuir*. 31, 7391–7400. doi:10.1021/la5046018
- Szymańska, K., Pudło, W., Mrowiec-Białoń, J., Czardybon, A., Kocurek, J., and Jarzębski, A. B. (2013). Immobilization of Invertase on Silica Monoliths With Hierarchical Pore Structure to Obtain Continuous Flow Enzymatic Microreactors of High Performance. *Microporous Mesoporous Mater.* 170, 75–82. doi:10.1016/j.micromeso.2012.11.037
- Tallarek, U., Leinweber, F. C., and Seidel-Morgenstern, A. (2002). Fluid Dynamics in Monolithic Adsorbents: Phenomenological Approach to Equivalent Particle Dimensions. *Chem. Eng. Technol.* 25, 1177–1181. doi:10.1002/1521-4125(20021210)25:12<1177::aid-ceat1177>3.0.co;2-v
- Turke, K., Meinusch, R., Cop, P., Prates da Costa, E., Brand, R. D., Henss, A., et al. (2021). Amine-Functionalized Nanoporous Silica Monoliths for Heterogeneous Catalysis of the Knoevenagel Condensation in Flow. *ACS Omega*. 6, 425–437. doi:10.1021/acsomega.0c04857
- Vervoort, N., Gzil, P., Baron, G. V., and Desmet, G. (2003). A Correlation for the Pressure Drop in Monolithic Silica Columns. *Anal. Chem.* 75, 843–850. doi:10.1021/ac0262199
- Yamada, T., Ogawa, A., Masuda, H., Teranishi, W., Fujii, A., Park, K., et al. (2020). Pd Catalysts Supported on Dual-Pore Monolithic Silica Beads for Chemoselective Hydrogenation under Batch and Flow Reaction Conditions. *Catal. Sci. Technol.* 10, 6359–6367. doi:10.1039/D0CY01442G

Conflict of Interest: The authors declare that the research was conducted in the absence of any commercial or financial relationships that could be construed as a potential conflict of interest.

Publisher's Note: All claims expressed in this article are solely those of the authors and do not necessarily represent those of their affiliated organizations, or those of the publisher, the editors, and the reviewers. Any product that may be evaluated in this article, or claim that may be made by its manufacturer, is not guaranteed or endorsed by the publisher.

Copyright © 2021 Jatoi, Goepel, Poppitz, Kohns, Enke, Hartmann and Gläser. This is an open-access article distributed under the terms of the Creative Commons Attribution License (CC BY). The use, distribution or reproduction in other forums is permitted, provided the original author(s) and the copyright owner(s) are credited and that the original publication in this journal is cited, in accordance with accepted academic practice. No use, distribution or reproduction is permitted which does not comply with these terms.